COMPARISON OF THE PERFORMANCES OF THREE STATE-OF-THE-ART OCEAN WAVE MODELS IN EXTREME STORM CASES

Roop Lalbeharry

Meteorological Service of Canada
Meteorological Research Branch
4905 Dufferin Street, Downsview
Ontario, Canada M3H 5T4

1. INTRODUCTION

In this study the three state-of-the-art third generation ocean wave models, namely, the wave model WAM, the model Wavewatch-III (hereinafter referred as WW3) and the near shore wave model SWAN are used to simulate wave height for two extreme storms which traversed the Canadian buoy network in the Northwest Atlantic during the periods 19-23 January 2000 and 12-16 January 2002, respectively, producing significant wave heights in excess of 9 m at some of the buoy locations. Wave height simulations using these models are done on two grids, namely, a coarse grid with a resolution of 0.5^o covering the area 25^oN - 70^oN and 80^oW - 15^oW and a fine grid with a resolution of 0.1^o nested within the coarse grid and covering the area 42^oN - 48^oN and 62^oW - 47^oW. The WAM and the WW3 model run on the coarse grid while the SWAN model and a nested version of the WAM run on the fine grid using the boundary conditions provided by the coarse grid WAM. The areas covered by the two grids and the locations of the buoys used in wave verification are shown in Fig. 1. The models are forced by winds generated by the Canadian Meteorological Centre (CMC) weather prediction model at three-hourly intervals and are spun up for a period of two days. The coarse grid winds drive both the coarse grid WAM and WW3 while the fine grid winds drive both SWAN and the nested version of the WAM. The primary objective of this study is to compare the performances of these models running in shallow water mode in extreme storm cases. The basic formulations of the three models are briefly described in section 2. Model results and discussions are presented in section 3 followed by summary and conclusions in section 4.

2. MODEL FORMULATIONS

2.1 Action Density Equation

The ocean waves are described with the two-dimensional wave action density spectrum $N(\sigma,\theta,\phi,\lambda,t)$ as a function of relative angular frequency σ, wave direction θ, latitude ϕ, longitude λ, and time t. The action density spectrum is defined as the energy density spectrum $F(\sigma,\theta,\phi,\lambda,t)$ divided by σ observed in a frame moving with the ocean current velocity, that is, $N(\sigma,\theta,\phi,\lambda,t) = F(\sigma,\theta,\phi,\lambda,t)/\sigma$. The action density is chosen because it is conserved in the presence of time-dependent water depths and currents whereas the energy density spectrum is not. In general, the conservation equation for N in flux form in spherical coordinates is given in the form:

$$\frac{\partial}{\partial t} N + (\cos\phi)^{-1} \frac{\partial}{\partial \phi}(c_\phi \cos\phi N) + \frac{\partial}{\partial \lambda}(c_\lambda N) + \frac{\partial}{\partial \sigma}(c_\sigma N) + \frac{\partial}{\partial \theta}(c_\theta N) = \frac{S}{\sigma} \quad (1)$$

where

$$S = S_{in} + S_{nl} + S_{ds} + S_{bf} + S_{br} \quad (2)$$

In (1) the first term on the left hand side represents the local rate of change of action density in time, the second and third terms the propagation of action density in geographical space (with propagation velocities c_ϕ and c_λ in

latitude

Fig. 1 Area covered by the coarse 0.5° x 0.5° grid. Enclosed box is the area covered by the fine or nested 0.1° x 0.1° grid. The locations of buoys used for validation are also shown.

Fig. 2. Storm tracks for (a) the period 20-22 January 2000 and (b) the periods 11-13 (Trk #2) and 13-15 (Trk #1) January 2002, respectively. The lower numbers give the storm's central pressures in hPa at the dates and times indicated. In the text the storm with track Trk #1 is referred to as Storm_T1 and that with

Trk #2 as Storm_T2.

and longitude space, respectively), the fourth term the shifting of the relative frequency due to variations in depths and currents (with propagation velocity c_σ in σ space) and the fifth term the depth-induced and current-induced refraction (with propagation velocity c_θ in θ space). The term $S = S(\sigma,\theta,\phi,\lambda,t)$ on the right hand side of (1) is the net source term expressed in terms of energy density. It is the sum of a number of source terms given in (2) representing the effects of generation (S_{in}), quadruplet and triad nonlinear wave-wave interactions (S_{nl}), dissipation due to whitecapping (S_{ds}), bottom friction (S_{bf}) and depth-induced wave breaking (S_{br}). S_{in} is described as the sum of linear and exponential growth in which the linear growth is due to Cavaleri and Malonette-Rizzoli (1981) but with a filter to eliminate contributions from frequencies lower than the Pierson-Moskowitz frequency, Tolman (1992). In deep and intermediate waters quadruplet nonlinear wave-wave interactions dominate the evolution of the spectrum so that in the WAM and WW3, S_{nl} consists only of these interactions and is computed with the discrete interaction approximation method as proposed by Hasselmann et al. (1985). On the other hand, in very shallow waters triad wave-wave interactions become very important so that in the SWAN model S_{nl} is made up of both quadruplet and triad wave-wave interactions and one or both interactions can be activated. The bottom friction source term S_{bf} follows the formulation of Hasselman et al. (1973) based on the results of the JONSWAP experiment. The bottom friction coefficient is set to 0.067 m^2s^{-3} for fully developed wave conditions or to 0.038 m^2s^{-3} for swell conditions. The depth-induced wave breaking source term S_{br} included here is due generally to the work of Battjes and Janssen (1978) in which the free parameter and the breaker parameter are set by the user.

2.2 The WAM

The WAM solves the energy balance form of (1) for no currents and fixed water depths for both deep and shallow waters on a spherical grid. WAMDI Group (1988) describes the Cycle-3 version of WAM (hereinafter referred as WAM3) in which S_{in} and S_{ds} are based on the formulations of Komen et al. (1984). In the current Cycle-4 version of WAM (hereinafter referred as WAM4), S_{in} and S_{ds} are based on the formulations of Janssen (1989, 1991) in which the winds and waves are coupled, that is, there is a feedback of growing waves on the wind profile. The effect of this feedback is to enhance the wave growth of younger wind seas over that of older wind seas for the same wind. It solves the wave propagation equation using the first order upwind explicit scheme which results in the propagation time step being limited by the CFL condition while the source term integration uses a semi-implicit scheme. More details of the formulation of the WAM can be found in Komen et al. (1994).

2.3 SWAN

The SWAN model solves the action balance equation on a spherical grid as an option. Because of the assumptions of time-independent water depths and no currents, the solution of (1) is equivalent to the solution of the energy balance equation as in WAM. However, it uses an implicit scheme to propagate the wave action density, which has the great advantage that the propagation time step is not limited by any numerical condition since the scheme is unconditionally stable in geographic and spectral space. In geographic space the scheme is first-order upwind and it is applied to each of the four directional quadrants of wave propagation in sequence (i.e., divided into four sweeps). In the spectral space the scheme is variable between an upwind scheme and a central scheme. The numerical scheme used for the source term integration is chosen by the user and can be the fully implicit, semi-implicit or explicit scheme. SWAN has the option of using WAM3 or WAM4 physics for the S_{in} and S_{ds} source terms. The version of the SWAN model used in this study is SWAN Cycle-3 version 40.11 (see SWAN User Manual, 2000; Booij et al., 1999; Ris et al.,1999).

2.4 WW3

As in SWAN the wave model WW3 also solves the action density balance equation but with a variable wavenumber coordinate k ($= 2\pi/L$, L being wavelength) replacing the wave coordinate σ. The propagation velocity c_k in wavenumber space replaces the propagation velocity c_σ in frequency space with the former closely resembling the latter (Tolman and Booij, 1998). With the assumption of no currents and fixed depths, $c_k = 0$ as in the case of c_σ. The solution of (1), therefore, simplifies to the solution of the energy balance equation as in the case of the WAM and SWAN. The S_{in} and S_{ds} source terms are based on the formulations of Tolman and Chalikov (1996) and includes also the option of using WAM3 physics for these source terms. In WW3 all the boundary points are set to land points. More details of the physics of WW3 version 1.18 and the numerical approaches used are described by Tolman (1999).

2.5 Model Assumptions and Configurations

It is assumed that there are no currents and that the water depths are time-independent. These assumptions lead to $c_\sigma = 0$, that is, σ is conserved. The fourth term on the left hand side of (1) vanishes and (1) reduces to the conservation equation for energy density $F(\sigma,\theta,\phi,\lambda,t)$ in flux form. It should be noted that in the cartesian coordinate system, the flow is divergent-free but not so in the spherical coordinate system. The assumption of no currents implies that refraction is due only to spatial variations of water depths. Further, since the models are applied to shelf seas and deep oceans in shallow water mode, the depth-induced wave breaking source term S_{br} in (1) and the SWAN triad nonlinear wave-wave interaction source term in S_{nl} are small and hence ignored. The bottom friction coefficient in S_{bf} is set to 0.067 $m^2 s^{-3}$. The solution of (1) is provided for 25 frequencies logarithmically spaced from 0.042 Hz to 0.41 Hz at intervals of $\Delta f/f = 0.1$ and 24 directional bands at 15° each, so that at each model grid point there are 600 spectral estimates at any given time. The configurations and other information of the coarse and fine grids are given in Table 1.

Table 1. Model configurations. The extensions "CG" and "FG" stand for coarse and fine grids, respectively. Note that the number of water points in WW3_CG is less than those in WAM4_CG since the boundary points in the former are treated as land points.

	WAM4_CG	WW3_CG	WAM4_FG	SWAN
Grid resolution:				
spatial $(\Delta\lambda \times \Delta\phi)$	$0.5^o \times 0.5^o$	$0.5^o \times 0.5^o$	$0.1^o \times 0.1^o$	$0.1^o \times 0.1^o$
spectral : frequency	25	25	25	25
direction	24	24	24	24
Grid dimensions	131 x 91	131 x 91	151 x 61	151 x 61
No. of grid points	11921	11921	9211	9211
No. of sea points	9289	9010	8608	8608
Wave physics	Shallow water	Shallow water	Shallow water	Shallow water
Time step: propagation	240 s	3600 s	120 s	20 min
source	240 s	300 s	120 s	20 min

3. RESULTS AND DISCUSSION

3.1 Storm Cases and Validation Buoys

Wave heights are simulated for extreme storm cases which occurred during the periods 19-23 January 2000 and 12-16 January 2002, respectively. The storm track for the former period is shown in Fig. 2a while the two storm tracks during the latter period are shown in Fig.2b, the primary track being the track denoted as "Trk #1". These storms underwent explosive development and can be considered as "bombs" since the central pressure fell by more than 24 hPa in a 24-hour period. The buoys used for validation of model results and their geographical locations are shown in Fig.1. Table 2 separates the validation buoys used for each of the storm cases and for each of the two grids. The buoy denoted as "RG3" is the oil rig called "Rowan Gorilla III"

3.2 19-23 January 2000 Storm Case

Fig. 3 presents a comparison of observed and model significant wave heights (SWH) at buoy locations RG3 with a water depth of 45 m and 44140 with a water depth of 90 m for the fine or nested grid (Fig. 3a) and the coarse grid (Fig. 3b). In the figure legends, WAM4(FGSH/CGSH) refers to results based on WAM4 fine/coarse grid and shallow water physics runs, SWAN(WAM4/WAM3) denotes SWAN nested grid results based on WAM4/WAM3 physics for S_{in} and S_{ds} and WW3(TC/WAM3) denotes WW3 coarse grid results based on Tolman and Chalikov/WAM3 physics for the S_{in} and S_{ds} source terms. In all the model runs, the times of occurrence of the peak wave heights are in good agreement with the observed times. In Fig. 3a the WAM4(FGSH) and SWAN(WAM3) results are quite comparable and in close agreement with the observations. The figure further shows that SWAN(WAM3) outperforms SWAN(WAM4), a result found also by Booij et al. (1999). These results are also quite similar to those obtained by Lalbeharry et al. (2001). At RG3 WAM4(FGSH) and SWAN(WAM3) generated peak SWH close to the observed peak of 12 m but at 44140 the major peak was underpredicted by about

1 m. In Fig. 3b WAM(CGSH) and WW3(WAM3) results compare well with the observed wave heights, especially at RG3. At 44140 the major peak of 9 m was also underpredicted by about 1 m as the in the case of WAM4(FGSH) and SWAN(WAM3) runs shown in Fig. 3a. A comparison of WAM4(CGSH) with WW3(TC) indicates that the WAM4
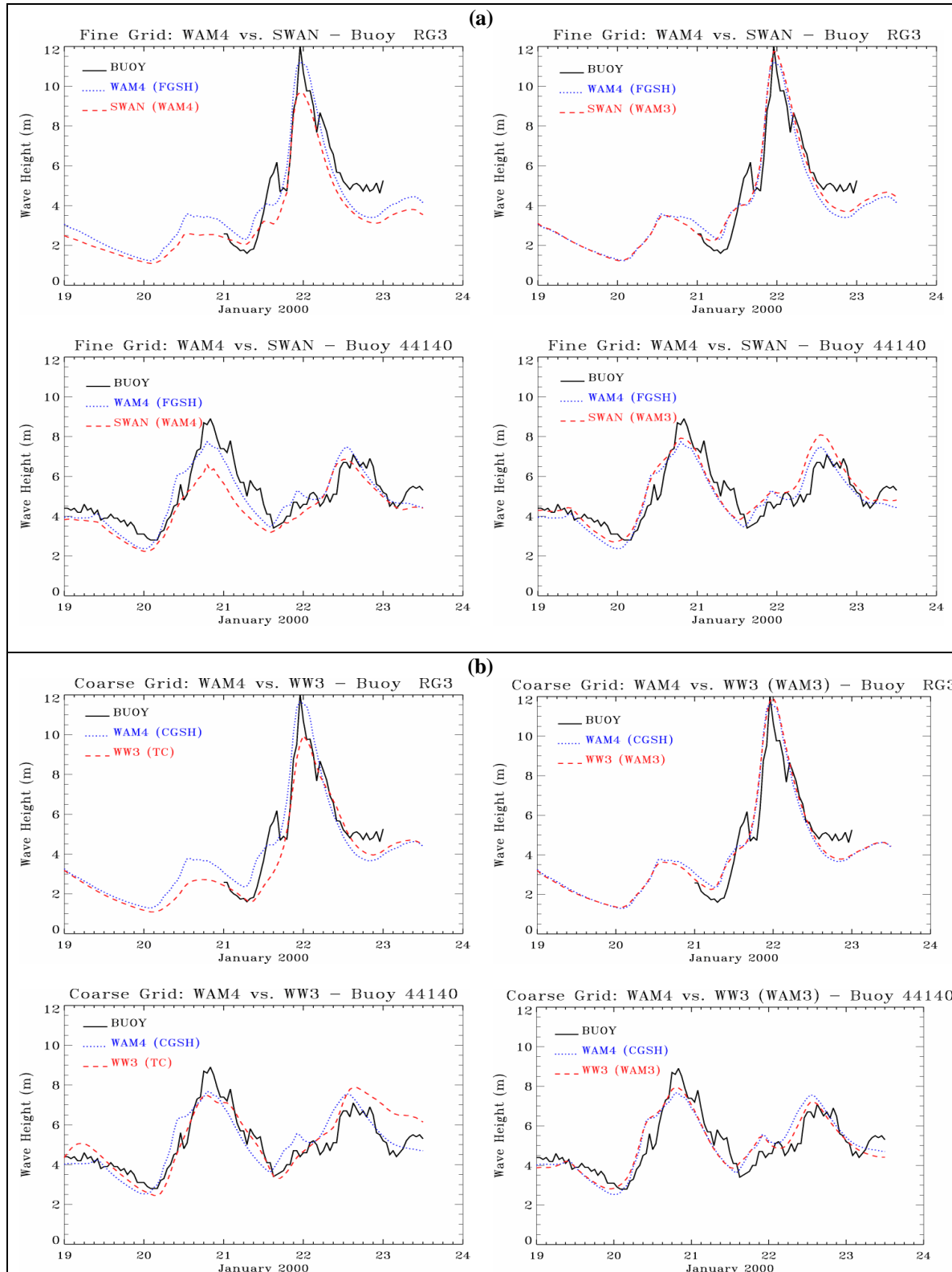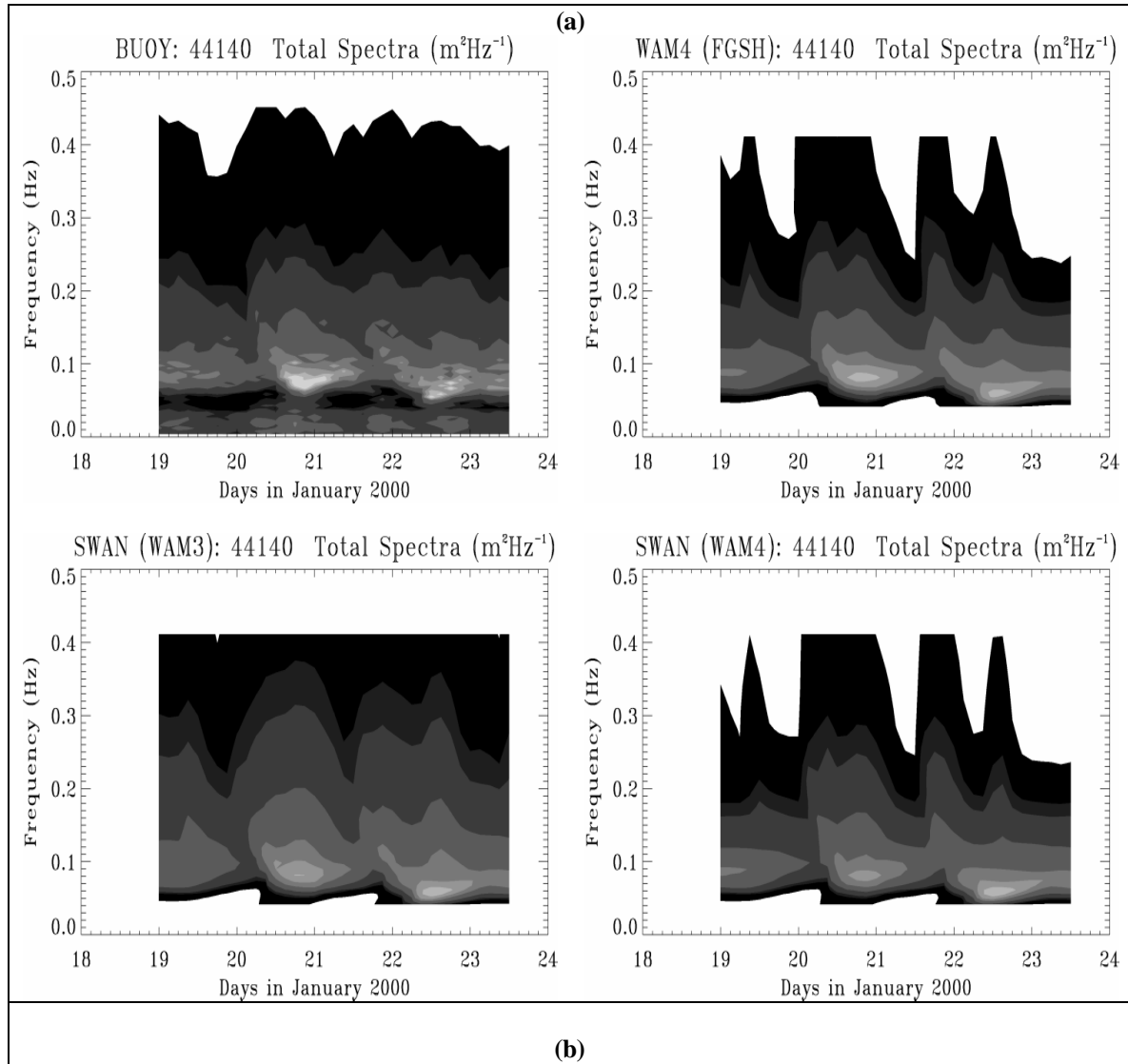
Fig. 3. Comparison of observed and model significant wave heights (SWH) at buoy locations RG3 and 44140 for (a) fine or nested grid and (b) coarse grid runs for the period 19-23 January 2000. See text for legend explanation.
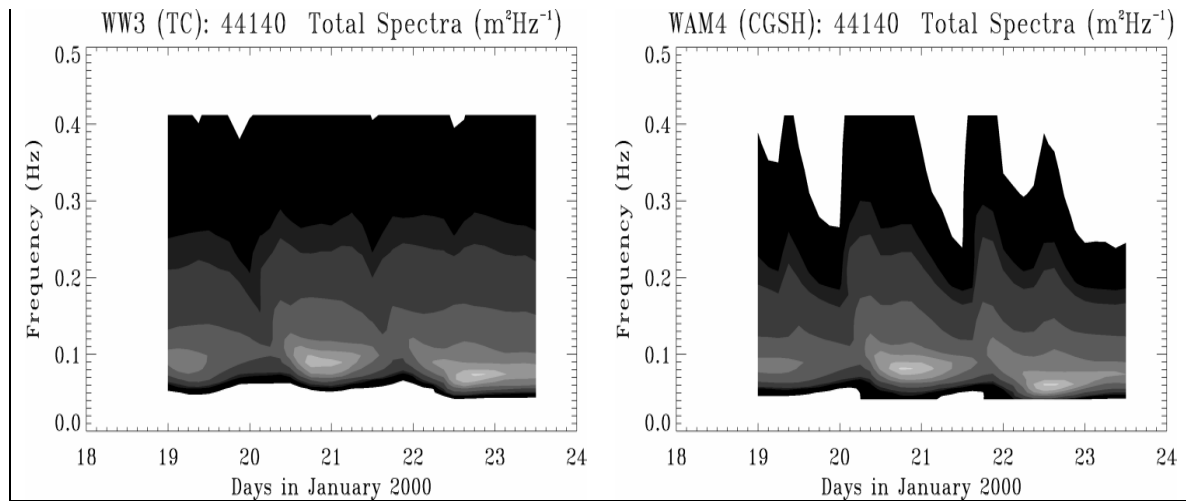

(a)

(b)

Fig. 4. Time series plots of the buoy and model one-dimensional (1d) spectra at 3-hourly intervals at the location of buoy 44140 for the period 19-23 January 2000. The gray scale contours correspond, respectively, to energy density levels of 0.05, 0.5, 1, 5, 20, 40, 70 and 100 m^2 Hz^{-1}.

improves the prediction of the peak SWH by about 1.5 m at RG3 while at 44140 the agreement is better for the major peak SWH and less so for the minor peak SWH. There is little or no difference between the WAM4(FGSH) and WAM4(CGSH) SWH and this seems to suggest that the impact of a higher resolution grid on the SWH at water depths of the buoys considered here is rather marginal.
.

Table 2. Buoys and their corresponding water depths used for validation of model results. The buoys used for validating the coarse and nested grids model results for each of the two storms are also shown.
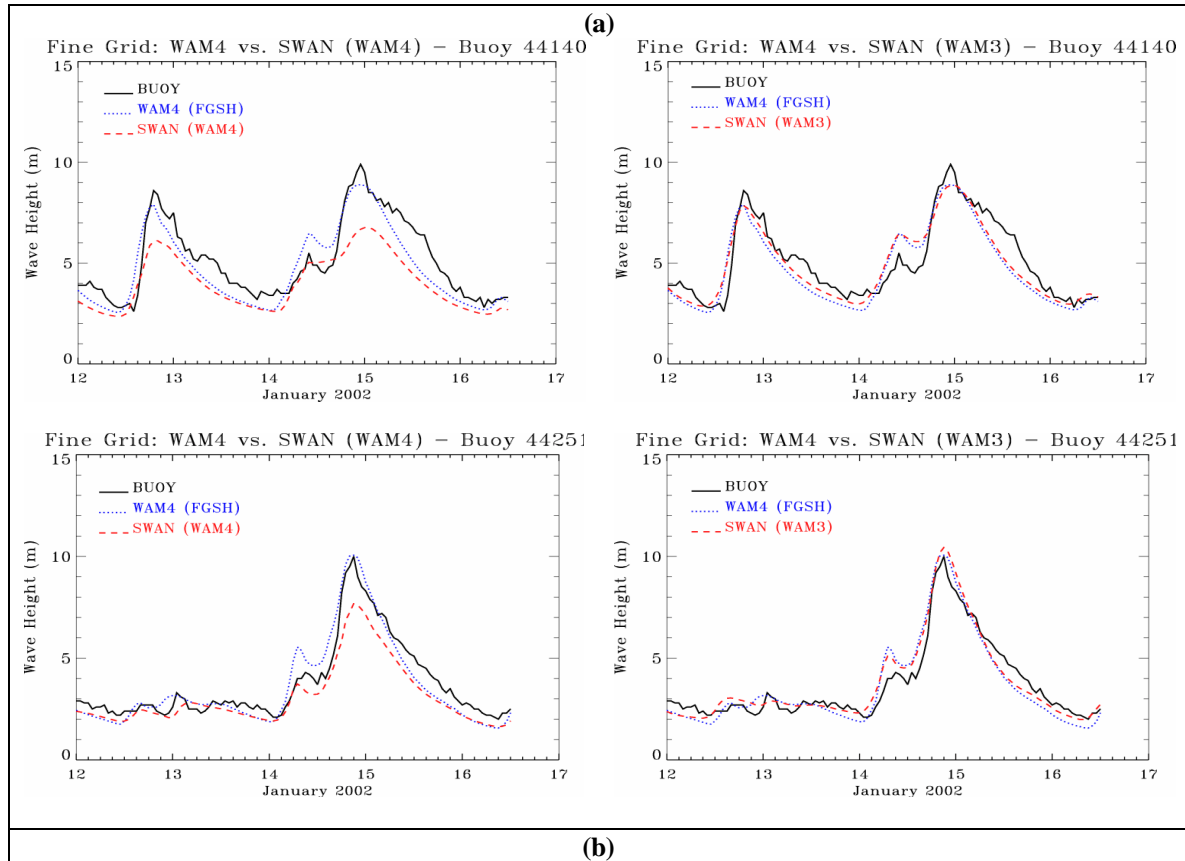
Buoys	Water Depths(m)	January 2000 Storm		January 2002 Storm	
		Coarse Grid	Nested Grid	Coarse Grid	Nested
44137	4500	44140	44140	44137	44140
44140	90	44141	44141	44140	44141
44141	4500	44255	44255	44141	44251
44142	1300	RG3	RG3	44142	
44251	71			44251	
44255	185			44255	
44258	58			44258	
RG3	45			44004	
44004	3164			44005	
44005	201			44008	
44008	63			44009	
44009	28			44025	
44025	40			41001	
41001	4389				

Fig. 4 presents time series plots of the buoy and model one-dimensional (1d) spectra at 3-hourly intervals in which the energy densities are contoured in terms of gray scales at the location of buoy 44140. This figure complements Fig. 3 in that there is one-to-one correspondence between peaks in SWH and 1d-spectra. The buoy spectra indicates the passage of two major storms at this location, one around 1800 UTC 20 January and the other around 1200 UTC 22 January with the former being more intense. Model peak spectral intensities are somewhat weaker than the corresponding buoy ones with model peak frequencies f_p close to 0.08 Hz (peak period T_p of 12.5 s) for the first storm and 0.06 Hz (T_p of 16.5 s) for the second storm compared with the observed f_p of 0.075 Hz (T_p of 13.3 s) and 0.055 (T_p of 18.2 s), respectively. For the first storm the SWAN(WAM3) and SWAN(WAM4) runs generate weaker peak spectral intensities than those generated by the WAM4(FGSH), WAM4(CGSH) and WW3(TC) while for the second storm the model runs show more comparable peak spectral intensities.

3.3 12-16 January 2002 Storm Case

Two explosive storms whose tracks and central pressures are shown in Fig. 2b moved through the Canadian waters during the period 12-16 January and generated wave heights in excess of 9 m at several buoy locations. The storm with track "Trk #1" will henceforth be referred as Storm_T1 while that with track "Trk #2" as Storm_T2. Fig. 5 presents model simulations of SWH compared against observations at selected buoys. The impact of the two storms was observed at buoy 44140 with the impact of Storm_T1 being the more dominant storm at buoys 44251, 44137 and 44008. The water depths of these buoys are given in Table 2. The results presented in Fig. 5 are quite similar to those presented in Fig. 3 for the January 2000 storm. At buoy 44140 in Fig. 5a, the models generated two major SWH peaks, one produced by Storm_T2 around 1900 UTC 12 January 2002 and the other by Storm_T1 around 0000 UTC 15 January 2002, both in close agreement with the observed times. The results show more specifically that the models did well in predicting the times of occurrence of the peak SWH although with varying degrees of intensities. SWAN(WAM3) again outperforms SWAN(WAM4) and is in good agreement with WAM4(FGSH) which in turn agrees well with the coarse grid WAM4(CGSH). In general, WAM4(CGSH) slightly outperforms WW3(TC) as shown in Fig. 5b although the agreement is much better for the Storm_T1 peak SWH at buoy 44140 around 0000 UTC 15 January 2002. The water depth of buoy 44140 is 90 m and that of 44251 is 71 m. A comparison of WAM4(FGSH) or SWAN(WAM3) with WAM4(CGSH) once again indicates that there is little or no impact on the SWH of a higher resolution model at these depths.

Fig. 6 is the same as Fig. 4 but for the period 12-16 January 2002. At buoy 44140 the 1d-spectra of all the models identify two major spectral peaks, one near 1800 UTC 12 January 2002 associated with Storm_T2 and a
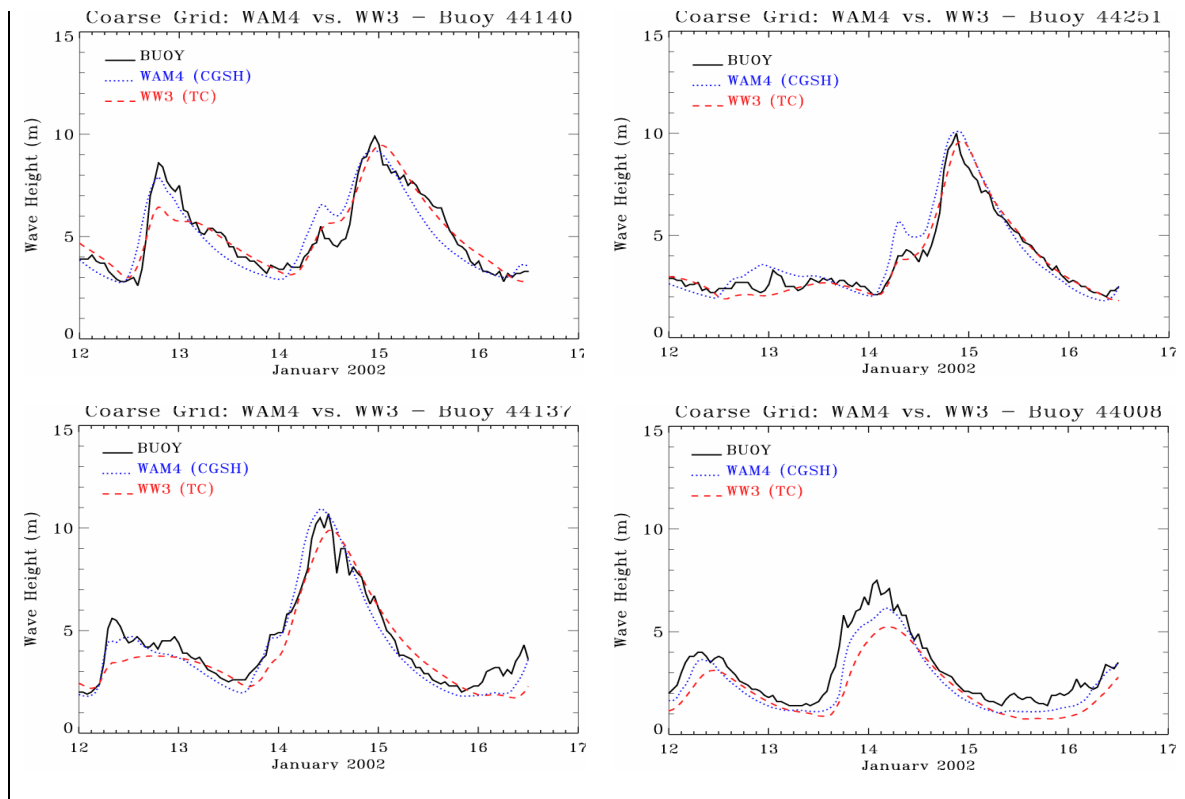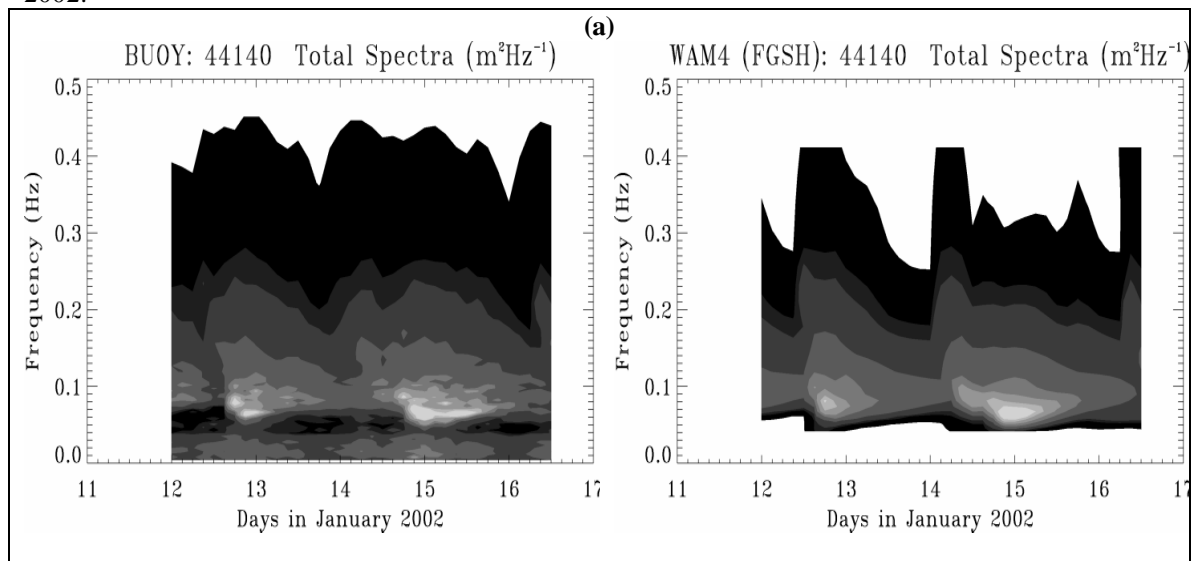

(a)

(b)

Fig. 5. Same as Fig. 3 but for buoy locations 44140, 44251, 44137 and 44008 and for the period 12-16 January 2002.
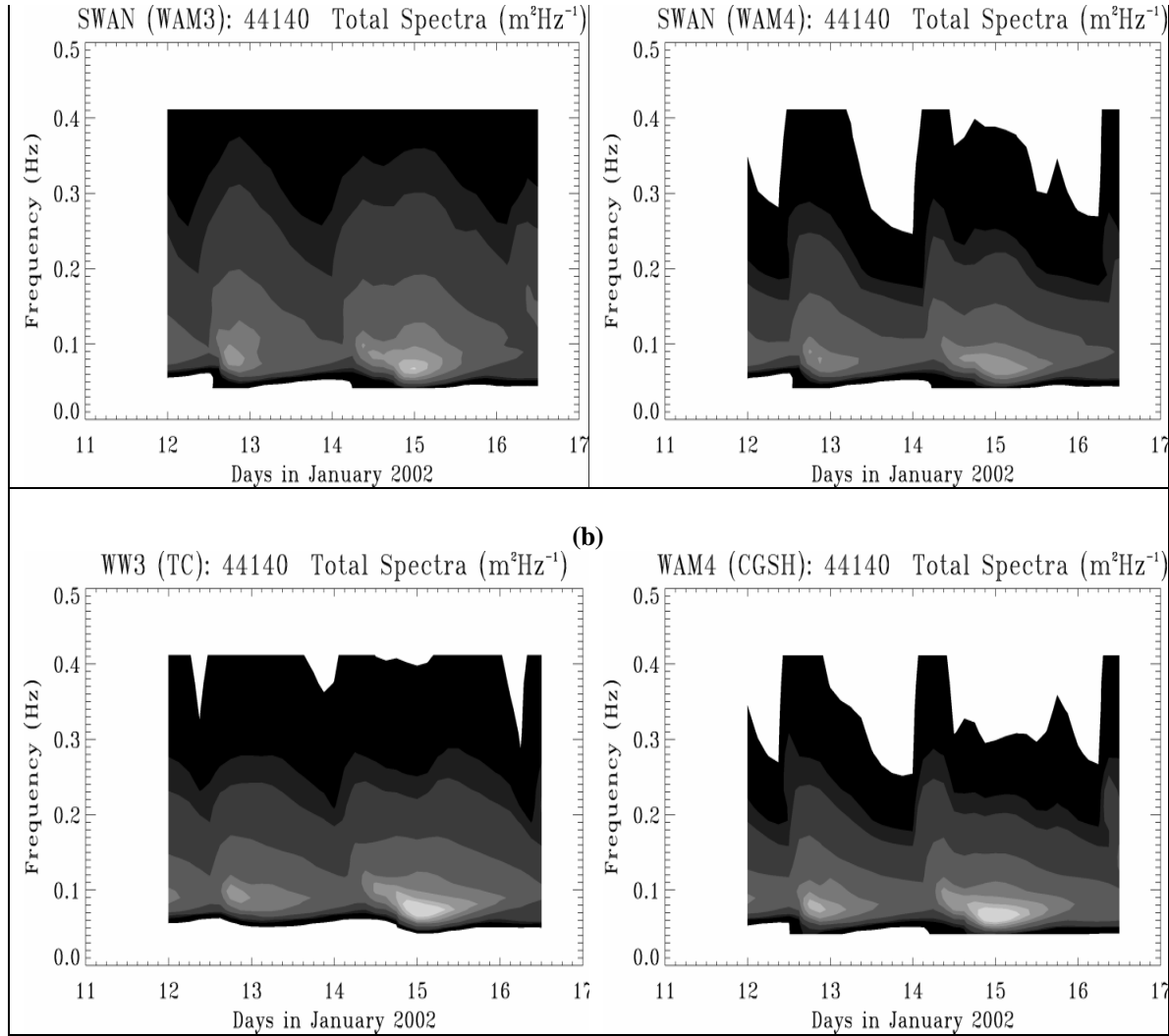
(a)

Fig. 6. Same as Fig. 4 but for the period 12-16 January 2002.

more intense one at 0000 UTC 15 January 2002 associated with Storm_T1 with f_p close to 0.06 Hz (T_p of 16.7 s), all in agreement with the buoy spectra. The buoy spectral intensities are somewhat stronger than the model intensities generated for these two storms. In the case of Storm_T1 the peak spectral intensities generated by the nested WAM4(FGSH) and SWAN(WAM3) and the coarse WAM4(CGSH) and WW3(TC) runs are quite comparable while the peak intensity generated by the SWAN(WAM4) run is weaker than that produced by the SWAN(WAM3) run as expected.

3.4 Composite Storm Statistics

The combined wave statistics for the two storm cases for each model run are presented in Table 3. It is clear from this table that for the coarse grid WAM4(CGSH) performs somewhat better than WW3(TC) for both wave heights and peak periods. In the case of the fine grid SWAN(WAM3) outperforms SWAN(WAM4) for wave heights but not so for peak periods. WAM4(FGSH) did slightly better than SWAN(WAM3) and the peak period statistics are more in line with those of SWAN(WAM4). WAM4(FGSH) is nested in WAM4(CGSH) and their statistics are close enough to suggest that the impact of the higher resolution grid at the water depths of the buoys used in the validation is rather marginal.

*Table 3: Wave statistics for the combined periods 19-23 January 2000 and 12-16 January 2002 for the different model runs using shallow water physics and the buoys given in Table 2. Here, **Bias = 1/n**$\bf{S}$**(X_i - Y_i) is*

the mean error, $\boldsymbol{Rmse = [1/N\boldsymbol{S}(X_i - Y_i)^2]^{1/2}}$ *the root mean square error,* **SI = Rmse/(Buoy Mean)** *is the scatter index, and* $\boldsymbol{r = [1/N\boldsymbol{S}(Y_i - mean\ Y)(X_i - mean\ X)]/\boldsymbol{s}_y\boldsymbol{s}_x}$ *the linear correlation coefficient, where* X_i *and* Y_i, *are, respectively, the* i^{th} *observed and model values,* $\boldsymbol{s}_y$ *the standard deviation of Y,* $\boldsymbol{s}_x$ *that of X and N the number of observations.*

Wave Height Statistics (m)					
	WAM4(CGSH)	WW3(TC)	WAM4(FGSH)	SWAN (WAM4)	SWAN(WAM3)
Buoy Mean	3.570	3.570	4.660	4.660	4.660
Model Mean	3.405	3.220	4.620	4.122	4.680
Bias	-0.165	-0.350	-0.040	-0.537	0.020
Rmse	0.739	0.838	0.836	1.209	1.060
SI	0.207	0.235	0.179	0.260	0.228
r	0.951	0.942	0.930	0.862	0.887
N (no. of obs.)	1684	1684	703	703	703
Peak Period Statistics (s)					
Buoy Mean	10.160	10.160	11.955	11.955	11.955
Model Mean	9.480	8.147	11.397	11.507	11.059
Bias	-0.680	-1.743	-0.558	-0.448	-0.897
Rmse	4.007	4.227	3.860	3.918	4.332
SI	0.394	0.416	0.323	0.328	0.362
r	0.539	0.561	0.365	0.344	0.249
N (no. of obs.)	1575	1575	703	703	703

4. SUMMARY AND CONCLUSIONS

The ocean wave models WAM4, WW3 and SWAN are used in wave simulations of extreme storms over the Northwest Atlantic during the selected periods 19-23 January 2000 and 12-16 January 2002, respectively. The WAM4 and WW3 run on a coarse grid while the SWAN and a nested version of WAM4 run on a fine grid using the boundary conditions provided by the coarse grid WAM4. All the models use shallow water physics, time-independent water depths and no currents and are forced by winds provided by the CMC weather prediction model. The model outputs of wave heights and peak periods are validated against available buoy observations.

The results of this validation indicate that SWAN using WAM3 physics performs better than SWAN using WAM4 physics. This confirms the findings of Booij et al. (1999) and Lalbeharry et al. (2001). However, the fine or nested grid WAM4 has a slight edge over SWAN using WAM3 physics. Further, the coarse grid WAM4 does a better job than the coarse grid WW3 using Tolman and Chalikov physics in simulating the extreme wave heights. The performance of WW3 using WAM3 physics is in close agreement with the coarse grid WAM4. Finally, the nested WAM4 produces wave statistics close to the coarse grid WAM4, suggesting the marginal impact of the high resolution grid on wave height simulations at water depths of the buoys used in the validation.

5. ACKNOWLEDGEMENTS

6. REFERENCES

Battjes, J. A. and J. P. F. M. Janssen, 1978: Energy loss and set-up due to breaking of random waves. Proc. 16th Intl. Conference on Coastal Engineering, Am. Soc. Civ. Eng., New York, 569-587.

Booij, N., R. C. Ris and L. H. Holthuijsen, 1999: A third generation wave model for coastal regions 1. Model description and validation. J. Geophy. Res., 104, C4, 7649-7666.

Cavaleri, L. and P. Malanotte-Rizzoli, 1981: Wind wave prediction in shallow water: Theory and applications. J. Geophys. Res., 86, 10961-10973.

Hasselmann, K., T. P. Barnett, K. Bouws, H. Carlson, D. E. Cartwright, K. Enke, J. I. Ewing, H. Gienapp, D. E. Hasselmann, P. Kruseman, A. Meerburg, P. Muller, K. Richter, D. J. Olbers, W. Sell and H. Walden, 1973: Measurements of wind-wave growth and swell decay during the Joint North Sea Wave Project (JONSWAP), Dtsch. Hydrogr. Z. Suppl., 12, A8, 95p.

Hasselmann, S., K. Hasselmann, J. H. Allender and T. P. Barnett, 1985: Computations and parameterizations of the nonlinear energy transfer in a gravity-wave spectrum. Part II: Parameterizations of the nonlinear transfer for application in wave models. *J. Phys. Oceanogr.*, **19**, 745-754.

Janssen, P. A. E. M., 1989: Wave-induced stress and the drag of air flow over sea waves *J. Phys. Oceanogr.*, **19**, 745-754.

———— , 1991: Quasi-linear theory of wind-wave generation applied to wave forecasting. *J. Phys. Oceanogr.*, **21**, 1631-1642.

Komen, G. J., L. Cavaleri, M. Donelan, K. Hasselmann, S. Hasselmann, and P. A .E. M. Janssen, 1994: Dynamics and Modelling of Ocean Waves, Cambridge University Press, Cambridge, 532p.

Lalbeharry, Roop, Weimin Luo and Laurie Wilson, 2001: A shallow water intercomparison of wave models on Lake Erie. Proc. 4th Int. Symp. on WAVES 2001, 2-6 September 2001, San Francisco, California, U.S.A. B. L. Edge and J. M. Hemsley (Eds), Am. Soc. Civ. Eng., pp. 550-559.

Ris, R. C., L. H. Holthuijsen and N. Booij, 1999: A third generation wave model for coastal regions 2. Verification. J. Geophy. Res., 104, C4, 7667-7681.

SWAN, 2000: User Manual SWAN Cycle III version 40.11, October 19, 2000. Delft University of Technology, Department of Civil Engineering, the Netherlands.

Tolman, H. J., 1999: User manual and system documentation of WAVEWATCH-III version 1.18. NOAA/NWS/NCEP/OMB Technical Note 166, 110pp.

———— , 1992: Effects of numerics on the physics in a third generation wind-wave model. J. Phys. Oceanogr., 22, 1095-1111.

———— , H. J. and D. V. Chalikov, 1996: Source terms in a wind wave model. J. Phys. Oceanogr., 26, 2497-2518.

———— and N. Booij, 1998: Modeling wind and waves using wavenumber-direction spectra and a variable wavenumber grid. The Global Atmosphere and Ocean System, 6,295-309.

WAMDI Group, 1988: The WAM model - A third generation ocean wave prediction model. J. Phys. Oceanogr., 18, 1775-1810.